Influence of condensed silica fume and sand/cement ratio on pore structure and frost resistance of Portland cement mortars

Feldman, R. F.

Publisher's version / Version de l'éditeur:

Publication - American Concrete Institute, N91, 2, pp. 973-989, 1986

National Research Council Canada
Institute for Research in Construction

Conseil national de recherches Canada
Institut de recherche en construction

Influence of Condensed Silica Fume and Sand/Cement Ratio on Pore Structure and Frost Resistance of Portland Cement Mortars

by R.F. Feldman

Reprinted from
"Fly Ash, Silica Fume, Slag, and Natural Pozzolans in Concrete"
Proceedings Second International Conference
Madrid, Spain, 1986
ACI, SP-91-47, Vol. 2, p. 973-989
(IRC Paper No. 1397)

Price $2.00

NRCC 26202

Canada

RÉSUMÉ

On a contrôlé par porosimétrie au mercure, durant une cure de 180 jours, la modification de la structure des pores dans des mortiers de ciment Portland contenant 0, 10 et 30 % de silice fine et ayant un rapport eau/liant de 0,60 et un rapport sable/ciment de 2,25. La valeur liminaire d'intrusion dans les pores augmente avec leur dimension et diminue avec l'ajout de silice fine; elle est de l'ordre de 0,5 à 20 × 10^3 nm.

On a également préparé des mortiers sans silice fine ou en contenant 10 % suivant un rapport eau/ciment de 0,60 et des rapports sable/ciment de 0, 1,0, 1,5, 1,8, 2,0, 2,25 et 3,0; le sable satisfaisait à la norme ASTM C109. Des mesures de la porosité par injection de mercure ont été effectuées après 14 jours de cure. En présence de silice fine, le volume des pores ayant un diamètre compris entre 0,5 et 20 × 10^3 nm a augmenté avec le rapport sable/ciment. Des prismes de mortier ont été soumis à de[illegible] h) conformémen[illegible]66 (procédure [illegible] au gel-dégel e[illegible]ds résiduels. [illegible]rt sable/ciment[illegible] à 0,02 % aprè[illegible]us faible, l'[illegible] protection.

SP 91-47

Influence of Condensed Silica Fume and Sand/Cement Ratio on Pore Structure and Frost Resistance of Portland Cement Mortars

by R. F. Feldman

Synopsis: Pore structure changes in silica fume-portland cement blend mortars fabricated with 0, 10 and 30% silica fume at a water/binder ratio of 0.60 and a sand/cement ratio of 2.25 have been monitored by mercury porosimetry while being cured for 1 to 180 days. The threshold value for pore intrusion increases with pore size and becomes less abrupt with silica fume addition; it is in the 0.5 to 20 x 10^3 nm region.

Mortars were also made with and without 10% silica fume at a water/cement ratio of 0.60 and sand/cement ratios of 0, 1.0, 1.5, 1.8, 2.0, 2.25 and 3.0; the sand passed ASTM C109. Mercury intrusion measurements were carried out after 14 days of curing. In the presence of silica fume pore volume in the 0.5 to 20 x 10^3 nm pore diameter range increased with sand/cement ratio. Mortar prisms were subjected to freezing and thawing cycles (two cycles in 24 h) according to ASTM standard test method C 666, Procedure B. Freezing and thawing resistance was monitored by measuring changes in residual length and weight. Results indicate that if the sand/cement ratio is 2.25 or over, expansion is less than 0.02% after 500 cyles. At lower sand/cement ratios 10% silica fume gives little protection.

Keywords: cements; freeze-thaw durability; mortars (material); porosity; portland cements; sands; silica.

Dr. Feldman has studied the durability of materials for over 27 years, his interest centering on mechanical properties and porosity. He has published over 95 papers, co-authored a book on concrete science, and contributed chapters to volumes on related subjects. He is a Fellow of the American Ceramic Society.

INTRODUCTION

When by-product materials such as condensed silica fume, fly ash, and blast furnace slag are mixed with portland cement and hydrated, they produce a pore structure more discontinuous and impermeable than that of hydrated portland cement paste (1-3). This has been related to the low $Ca(OH)_2$ content of the hydrated blend product and it has been suggested that boundaries between the C-S-H phase and $Ca(OH)_2$ crystals, and perhaps $Ca(OH)_2$ crystals themselves, provide pathways for flow of fluids that are affected by the additives (1,2).

Microstructural changes in mortars (4) and preferential deposition of $Ca(OH)_2$ in the interfacial zone around aggregates (5,6) have been observed. It would therefore be expected that varying the sand/cement ratio (i.e., changing the amount of sand-paste interface) would influence the microstructure of the mortar. In addition, silica fume is a very reactive pozzolan and its presence in mortars might be expected to cause significant changes in the microstructure.

Recent work on mortars (7,8) and concrete (9) suggests that their frost resistance is improved by incorporation of silica fume. Although there is no strong indication of the mechanism, it has been postulated that a fine pore structure produced in the mortar by the silica fume renders the water unfreezable (7). Further work has indicated, however, that the pore structure is not so fine as was first thought (8).

It is the purpose of the present work to monitor the development of pore structure in mortars with and without silica fume and to investigate the effect of the sand-paste interface on the microstructure and frost resistance of the mixes.

EXPERIMENTAL

Materials

Type I portland cement with C_3A content of 11.8% (calculated by Bogue formula) and silica fume containing 95.2% SiO_2, 1.6% carbon, 0.27% K_2O and 0.10% Na_2O (surface area by N_2 adsorption 21 000 m^2/kg) were used. Ottawa silica sand meeting ASTM C109 was used for making mortars to give sand/binder ratios of 0, 0.5, 1.0,

1.5, 1.8, 2.0, 2.25 and 3.0. Most mixes were prepared at a w/(c+sf) of 0.60; two were prepared at a w/(c+sf) of 0.70. Binder in the mortar contained 0, 10 or 30% silica fume. No water-reducing or air-entraining admixtures were included.

Mixing

Cement, silica fume, and water were mixed together in the bowl of a Hobart Model N-50 mixer (ASTM C305) for 30 s at low speed. All the sand was added and mixing continued at low speed for another 30 s. The machine was stopped a second time, then mixing was continued at medium speed for 30 s. Mixing was stopped again for 1½ min, then resumed for 1 min more at medium speed. Mortar specimens were made in the form of 25.4 × 25.4 × 127-mm prisms outfitted with steel studs and were cured for 14 days.

Measurements

Pore size distribution -- This was determined by Hg intrusion porosimetry to 414 MPa. Specimens were dried in vacuum and then heated for about 15 h at 100°C. Measurements were made on:

1) Mortars containing 0, 10 or 30% silica fume (designated C^H, B^H_{10} and B^H_{30}, respectively) with a sand/cement ratio of 2.25, mixed at a w/(c+sf) of 0.60. Determinations were made at 1, 3, 7, 14, 28, 90 and 180 days of hydration.
2) Two series of mortars without silica fume. Series A, with sand/cement ratios of 0, 0.5, 1.0, 1.5, 1.8, 2.0, 2.25 and 3.0, was cured for 14 days at a w/(c+sf) of 0.60. Series B, with sand/cement ratios of 0, 1.5, 1.8, 2.0, 2.25 and 3.0, was cured for 28 days at a w/(c+sf) of 0.60.
3) A series of mortars containing 10% silica fume with sand/cement ratios of 0, 0.5, 1.0, 1.5, 1.8, 2.0, 2.25 and 3.0. This series was cured for 28 days at a w/(c+sf) of 0.60.
4) Two mortars containing 0 and 10% silica fume with sand/cement ratio of 3.0. These were cured for 28 days at a w/(c+sf) of 0.70.

Re-intrusion of mercury -- Hg was removed from specimens on which mercury intrusion experiments had been performed by heating them at 105°C in vacuum for several weeks until the weight returned to its initial value before intrusion. Re-intrusion was then performed on the specimens containing silica fume at sand/cement ratios of 0, 1.5, 1.8, 2.0, 2.25 and 3.0.

Freezing and thawing resistance -- This was determined for all mixes after 14 days of curing by two methods: 1) Residual expansion was measured, four specimens per mix; mortars were made in the form of 25.4 × 25.4 × 127-mm prisms outfitted with steel studs; the freeze-thaw cycle consisted of freezing in air and thawing in water (-18°C to +5°C), two cycles in 24 h. Cooling ratios were those of ASTM Standard Test Method C-666, Procedure B. 2) Weight loss was measured using mixes at a w/(c+sf) = 0.60, sand/cement ratio of 1.8, 2.0, 3.0, with and without 10% silica

fume, and at a w/(c+sf) = 0.70, sand/cement ratio of 3.0, with and without 10% silica fume.

RESULTS

Pore-size Distribution

Mortars with and without silica fume as a function of time -- The pore-size distribution of mortars made at a sand/cement ratio of 2.25, containing 0, 10 or 30% silica fume and cured for 1, 3, 7, 14, 28, 90 and 180 days at a w/(c+sf) of 0.60, are shown in Figure 1(a-c). The mortar mix without silica fume in Figure 1a displays a progressive decrease in total porosity with curing time. Porosity down to 100 nm pore diameter at 180 days is about 3%; a similar paste cured for only 28 days is less than 1.5% (10). Below a pore size of 100 nm the curves at all ages of curing are concave to the abscissa. (This is in contrast to pore distributions for specimens containing silica fume as referred to below.)

The mortar with 10% silica in Figure 1b displays less progressive behaviour, although below 60 nm the total intruded volume generally decreases as curing time increases. After three days the curves below 100 nm become convex to the pore diameter axis. This trend is similar to that observed previously in fly ash and slag blends, where it was related to disruption of discontinuous pores by high pressure intrusion and to the extent of the reaction of $Ca(OH)_2$ (11). A plot of the slope of the curves at the limit of the intrusion, dV/d log D (%/nm)10, versus age of curing is presented in Figure 2. There is a large increase in slope with time for specimens in which $Ca(OH)_2$ is decreasing or low, e.g., B^H_{30} and B^H_{10}. At about 150 nm the curves in Figure 1b for 7 to 180 days of curing merge, having the same pore volume of about 6%; above 150 nm the pore volume for 180 days is greater than that for the 7-day cured specimen.

The pore-size distribution curves for mortar with 30% silica fume in Figure 1c show the same trend as the curves for 10% silica fume. In the 100 to 4000 nm range the total pore volume is in many cases greater for specimens cured for longer lengths of time. The 3-day cured specimen has the lowest porosity down to a pore size of about 600 nm. At a pore size of about 30 nm the total intruded volume decreases with age of curing, and with ages greater than three days the curves are convex to the abscissa.

A comparison of the pore-size distribution curves reveals that the threshold value for pore intrusion (the point at which a large increase in intrusion occurs) increases with pore size (0.5 to 30×10^3 nm) and becomes less abrupt with additon of silica fume. These effects for mortars containing silica fume are usually accompanied by abrupt changes.

Mortars without silica fume -- Results for pore-size distribution of mortars at sand/cement ratios of 0, 1.5, 1.8, 2.0, 2.25 and 3.0, cured for 28 days (Series B) without silica fume

addition at a water/cement ratio of 0.60 are presented in Figure 3. Pore volume is based on the volume of the paste portion of the specimen. This is calculated by computing the volume of the individual components of the mix, based on density; the sand volume is subtracted from the total volume of the original mixture. The total porosity at 2.9 nm pore diameter now increases approximately with sand/cement ratio, the highest and lowest porosities being 40.5 and 35.6% for the 3.0 and 0 sand/cement ratios, respectively. The distribution of pores is vastly different, however; for a sand/cement ratio of 0.0 the pore volume down to 40 nm is only about 2.5%, while this value increases to 12, 19.5, 18.9, 20.5 and 21.2% for sand/cement ratios of 1.5, 1.8, 2.0, 2.25 and 3.0, respectively.

The measurement of pore-size distribution for mortars without silica fume was repeated in Series A, cured for 14 days; these mortars contained sand/cement ratios of 0, 0.5, 1.0, 1.5, 1.8, 2.0, 2.25 and 3.0. The results for the volume of coarser pores of diameter $(97 \rightarrow 0.875) \times 10^3$ nm are presented in Figure 4, together with the volume of this pore range for Series B. With some deviation in the 1.8 to 2.25 sand/cement ratio range, the pore volume usually increases with sand/cement ratio and is generally greater for the 14-day cured specimens.

Mortars containing silica fume, first intrusion -- The pore-diameter distribution of mortars containing 10% silica fume (cured for 28 days) with sand/cement ratios of 0.0, 0.5, 1.0, 1.5, 1.8, 2.0, 2.25 and 3.0 are presented in Figures 5 and 6; pore volume calculations are based on paste portion. Pore-size distribution results for the mortars without silica fume and re-intruded distributions for mortars with silica fume are also included.

The pore volume is divided into four ranges of pore diameter: $(97 \rightarrow 0.875)$, $(0.875 \rightarrow 0.175)$, $(0.175 \rightarrow 0.0175)$ and $(0.0175 \rightarrow 0.0029) \times 10^3$ nm. Figure 5 contains the results for sand/cement ratios of 0, 0.5, 1.0 and 1.5, and Figure 6 those for sand/cement ratios of 1.8, 2.0, 2.25 and 3.0. Addition of silica fume increases the volume of pores in the $(97 \rightarrow 0.875) \times 10^3$ nm range at all sand/cement ratios, an effect that increases with ratio; at one of 3.0, volume increases from approximately 4 to 10.5%. Generally, with silica fume addition the volume of pores in ranges $(97 \rightarrow 0.875) \times 10^3$ and $(0.875 \rightarrow 0.175) \times 10^3$ (the coarse ranges) and $(0.0175 \rightarrow 0.0029) \times 10^3$ nm (the finest range) increases and decreases in the $(0.175 \rightarrow 0.0175) \times 10^3$ nm range.

Mortars containing silica fume, re-intrusion -- The pore diameter distribution, on re-intrusion, for mortars containing 10% silica fume with sand/cement ratios of 0.0, 1.5, 1.8, 2.0, 2.25 and 3.0 are shown as histograms in Figures 5 and 6; the complete distributions are shown in Figure 7. There is an increase in the volume of $(97 \rightarrow 0.875) \times 10^3$ nm range pores compared to that at first intrusion, the increase being greater the larger the sand/cement

ratio. The volume of the two ranges of smallest pores is generally lower on second intrusion.

The complete range of pore size distribution in Figure 7 shows the effect of both first and second intrusion on the same plot. The hysteresis between the two curves increases with sand/cement ratio up to 2.0. Beyond this it decreases because specimens with sand/cement ratios of 2.25 and 3.0 already have relatively high pore volumes in the coarse ranges on first intrusion as well as larger pore volumes in the finer ranges.

A comparison of pore-size distributions from the re-intrusion for specimens with silica fume and the results from the first intrusion for the equivalent specimens without silica fume shows that the volume of the pore range (97→0.875) × 10^3 nm is larger on re-intrusion. The rest of the distribution is similar: the (0.0175→0.0029) × 10^3 nm range is slightly larger, the (0.175→0.0175) × 10^3 nm range is less, and the (0.875→0.175) × 10^3 nm is generally about the same.

Mortars with and without silica fume, w/(c+sf) = 0.70 and sand/cement ratio = 3.0 -- The pore-size distribution in this mortar is characterized by the high volume of pores in the (97→0.875) × 10^3 nm range, even without silica fume (about 13%). In both cases, with and without silica fume, the difference between pore volumes on first and second intrusion in the (97→0.875) × 10^3 nm range is not large.

Freezing and thawing resistance -- A summary is presented in Table I of results of residual expansion measurements on freezing and thawing cycle exposure. For comparison, column 7 gives the average percentage residual expansion per 100 freezing and thawing cycles × 100. Values are very high for specimens with and without silica fume until the sand/cement ratio is greater than 2.0 at a (w/(c+sf) = 0.60. Values for specimens with sand/cement ratios of 2.25 and 3.0 (w/(c+sf) = 0.60), 10% silica fume, are 0.26 and 0.16, respectively, while the values for the same mixes without silica fume are 102.5 and 0.68, respectively. The low value of the latter sample may be due not only to an increase in volume of pores of the (97→0.875) × 10^3 nm range but also to an increase in restraint to length change due to higher volume fraction of sand. Results of weight change with freezing and thawing of this mortar displayed large and rapid deterioration.

The mixes prepared at a w/(c+sf) of 0.70 with sand/cement ratio of 3.0 give average percentage residual expansion per 100 freeze-thaw cycles × 100 of 0.64 and 7.72 for mixes containing 0 and 10% silica fume, respectively. Both specimens lose a substantial amount of weight during cycles of freezing and thawing, but as shown in Table II that without silica fume loses weight more rapidly.

The results of weight loss for mortars made at w/(c+sf) = 0.60 and sand/cement ratios of 1.8 and 2.0 are similar to those in which

residual length change was measured; severe, rapid deterioration was indicated for specimens with and without silica fume. The mortar with sand/cement ratio of 3.0 and 10% silica fume showed no weight loss even after 548 cycles; without silica fume the mortar displayed large and rapid weight loss despite a low average residual length change measurement.

DISCUSSION

The marked difference in the pore-size distribution of pastes in mortars as a function of sand/cement ratio appears to be an interfacial effect. A preferential deposition of $Ca(OH)_2$ in the interfacial zone (less than 50×10^3 nm) around aggregates in concrete and mortars and around fibres in paste has been observed (5,6). The strength of mortars without silica fume is significantly less than that of paste after 14 days, when large quantities of $Ca(OH)_2$ have formed (4). In specimens containing silica fume a large proportion of the $Ca(OH)_2$ has reacted at this stage (4). After 28 days the strength development curves for both mortar and paste containing 30% silica fume diverge, the mortar becoming stronger. This has been attributed to the formation of a better bond between sand grains owing to new CSH formed from the reaction of $Ca(OH)_2$ and silica fume (4).

The development of pore structure leads to similar conclusions (Figure 1). The pore structure in mortars between 3 and 14 days shows lower values of pore volume than that in mortars cured for longer periods (size ranges 100-3000 nm). This may be because the lime concentration around each sand grain forms an initial structure; a subsequent structure resulting from a new CSH formation, by reaction between silica fume and this lime, may dominate the pore structure in the 100-3000 nm range. The abrupt increases in intruded volume suggest that rupture of the pore structure may occur in this region of mercury pressure. Such a rupture takes place at higher pressures in these blends as well as in hydrated fly ash and slag (1,11). The abrupt increases in intruded volume at intermediate pressures have not been observed in cement pastes, but only in mortars containing silica fume (10). The pore-size distribution of mortars without silica fume changes progressively. This (Fig. 1a) supports the assumption that differences in pore distribution in mortars with and without silica fume are not due solely to phenomena produced by the drying technique prior to mercury intrusion.

Formation of CSH at the interface of sand grains is not the only process that occurs. As has been shown in this and other work (12), a larger volume of pores in the $(97 \rightarrow 0.875) \times 10^3$ nm range is formed when the amount of interface per volume of specimen increases. These pores may be part of the duplex film observed (6) around interfaces owing to a possible reduction in the degree of hydration relative to that in mixes without sand (a result of reduction in permeability of the hydrate product as part of $Ca(OH)_2$ is segregated around sand grains (5)).

The presence of silica fume in mortar enhances the interfacial effects; some of the $Ca(OH)_2$ crystallized around sand grains can re-dissolve to react with relatively insoluble silica in locations relatively remote from the interface. This could explain further increase in volume of pores in the size range $97 \rightarrow 0.875 \times 10^3$ nm with addition of silica fume. The pore volume also increases with sand/cement ratio.

Properly entrained air creates frost-resistant concrete. Air-entrained bubbles are usually over 10×10^3 nm in diameter and the distance between them should be less than 0.2 mm. The bubbles must remain unsaturated with water to be effective, so that they must be relatively inaccessible to water migrating from the outside. Pores that form at or near the interface of sand grains are smaller than normal air-entrained bubbles, but some workers have concluded that pores down to 0.3×10^3 nm can improve the resistance of mortars to frost action (13). In addition, for sand/cement ratios of 2.25 or greater in a homogeneous mix, the average separation of pores formed at the interface would be less than 0.2 mm (8). The greater the sand content, the smaller the space between sand grains and the closer the pores to each other.

Addition of silica fume greatly decreases the permeability of mortars and concretes and ensures that a portion of the pores in the $(97 \rightarrow 0.875) \times 10^3$ nm range is relatively inaccessible even to mercury intrusion. As a consequence, pore volume in this size range increases on second mercury intrusion due to disruption of pore structure at high Hg pressures on first intrusion. This property is probably responsible, at least in part, for the improved frost resistance of mixes containing 10% silica fume at sand/cement ratios of 2.25 and 3.0 and w/(c+sf) of 0.60. Mortar containing silica fume, made at a w/(c+sf) of 0.70 and sand/cement ratio of 3.0, is not durable however, although it possesses a large pore volume in the $(97 \rightarrow 0.875) \times 10^3$ nm range accessible to mercury on first intrusion. This is probably due to the accessibility of the pores to water.

The pores in the $(97 \rightarrow 0.875) \times 10^3$ nm range formed at the interface of the sand grain can act as air-entrained bubbles, providing protection for mortars against frost action. The sand grains must be close enough together, however, to provide close spacing of pores, and the sand content must be high enough to provide sufficient pore volume. The presence of silica fume provides relative inaccessibility of these pores to water migrating from the outside.

CONCLUSIONS

1. Silica fume affects the pore-size distribution of mortars by reacting with the $Ca(OH)_2$ formed around sand grains as well as with the $Ca(OH)_2$ dispersed throughout the hydrated cement. This takes place within 28 days.
2. Pores in the $(97 \rightarrow 0.175) \times 10^3$ nm range are formed at the interface of sand aggregates in mortars. The pores increase

with sand-cement ratio in all mixes, with and without silica fume.

3. The pore-size distribution of mortars containing silica fume differs from that of equivalent mortars without silica fume by having a larger coarse pore component. Relative inaccessibility of these pores is due to a discontinuous pore structure, and this is responsible for the artificially large, fine-pore structure observed on first intrusion.
4. Frost resistance (according to ASTM C-666, Procedure B, at two freezing-thawing cycles a day) is increased by the addition of 10% silica fume to mortar with a w/(c+sf) = 0.60 when the sand/cement ratio is 2.25 or over. (The sand used is that passing ASTM C109. These results may not be applicable to normal concrete).
5. Improvement in frost resistance as a result of increase in the sand/cement ratio is due to pores in the range $(97 \rightarrow 0.875) \times 10^3$ nm formed at sand-matrix interfaces and their closer spacing.
6. Relative inaccessibility of pores contributes to frost resistance. This can be provided by the impermeable structure formed in the presence of silica fume.

ACKNOWLEDGEMENT

The author wishes to thank G.W. Chan for valuable help in performing the experiments. This paper is a contribution from the Division of Building Research, National Research Council of Canada.

REFERENCES

1. Feldman, R.F., "Significance of porosity measurements on blended cement performance"; Proceedings, 1st International Conference on Use of Fly Ash, Silica Fume, Slag and Other Mineral By-products in Concrete, Montebello, Canada, V. 1, SP-79, 1983, pp. 415-484 (Editor: V.M. Malhotra).

2. Feldman, R.F. and Huang Cheng-yi, "Microstructural properties of blended cement mortars and their relation to durability," RILEM Seminar on Durability of Concrete Structures under Normal Outdoor Exposure, Hanover, Germany, 1984.

3. Regourd, M., Mortureux, B., Aitcin, P.C. and Pinsonneault, P., "Microstructure of field concretes containing silica fume," Proceedings, 4th International Conference on Cement Microscopy, Las Vegas, U.S.A., 1982, pp. 249-260 (Editor: G.R. Gouda).

4. Huang Cheng-yi and Feldman, R.F., "Influence of silica fume on the microstructural development in cement mortar," Cement and Concrete Research, V. 15, No. 2, 1985, pp. 285-294.

5. Mikhail, R.Sh. and Youssef, A.M., "Studies on fibre-reinforced portland cement pastes, I. Surface area and pore structure,"

Cement and Concrete Research, V. 4, 1974, pp. 869-880.

6. Barnes, B.D., Diamond, S. and Dolch, W.L., "Micromorphology of the interfacial zone around aggregates in portland cement mortar"; Journal of the American Ceramic Society, V. 62 (1-2), 1979, pp. 21-24.

7. Traetteberg, A., "Frost action of blended cement with silica dust," Durability of Building Materials and Components, ASTM, STP 691, 1980, pp. 536-548.

8. Huang Cheng-yi and Feldman, R.F., "Dependence of frost resistance on the pore structure of mortar containing silica fume." In Press.

9. Sorensen, E.V., "Freezing and thawing resistance of condensed silica fume concrete exposed to deicing chemicals," Proceedings, 1st International Conference on Use of Fly Ash, Silica Fume, Slag and Other Mineral By-products in Concrete, ACI SP 79, V. II, 1983, pp. 709-713.

10. Feldman, R.F. and Huang Cheng-yi, "Properties of portland cement-silica fume pastes. I. Porosity and surface properties," Cement and Concrete Research, V. 15, No. 5, 1985, pp. 765-774.

11. Feldman, R.F., "Pore structure damage in blended cements caused by mercury intrusion," Journal of the American Ceramic Society, V. 62, No. 1, 1984, pp. 30-33.

12. Feldman, R.F., "The effect of sand-cement ratio and silica fume on the microstructure of mortars". In Press.

13. Litvan, G.G., "Air entrainment in the presence of superplasticizers," ACI Journal, Proceedings V. 80, No. 4, 1983, pp. 326-331 (Discussion in ACI Journal, Proceedings V. 8, No. 3, 1984, pp. 305-309).

TABLE I- Values for Residual Length Change Due to Exposure to Freezing and Thawing Cycles

Specimen		Cycles Producing		Ultimate	Ultimate	% Expansion
Sand/ Cement	Silica Fume	0.1 % Residual	0.2 Expansion	Expansion %	No. Cycles	per 100 cycles x 100
1	2	3	4	5	6	7
w/(c+sf) = 0.60						
3.0	0%	>470	>470	0.032	470	0.68
3.0	10%	>554	>554	0.009	554	0.16
2.25	0%	27	51	1.312	128	102.5
2.25	10%	>1486	>1486	0.039	1486	0.26
2.0	0%	48	76	0.220	80	27.5
2.0	10%	34	44	0.793	74	107.2
1.8	0%	31	52	0.470	82	57.3
1.8	10%	25	30	0.866	52	166.5
1.5	0%	5	10	0.833	36	231.4
1.5	10%	27	31	0.851	50	170.2
1.0	0%					
1.0	10%	2.9	33	0.846	50	169.2
0.5	0%					
0.5	10%	38	44	0.255	48	53.1
0.0	0%	11	16	0.200	16	125
0.0	10%	31	38	0.313	40	78.3
w/(c+sf) = 0.70						
3.0	0%	>204	>204	0.013	204	0.64
3.0	10%	138	Failed	0.122	158	7.72

TABLE II- Values for Weight Loss Due to Exposure to Freezing and Thawing Cycles

Specimen		Cycles Producing % Weight Loss		Ultimate Weight Loss %	Ultimate No. Cycles	% Weight Loss per 100 cycles x 100
Sand/ Cement	Silica Fume	0.5	2.0			
1	2	3	4	5	6	7
w/(c+sf) = 0.60						
3.0	0%	80	130	10.58	454	233.0
3.0	10%	>548	>548	0.0	548	0.0
2.0	0%	49	64	5.49	80	686.3
2.0	10%	53	58	9.04	66	1369.7
1.8	0%	55	62	7.37	82	898.8
1.8	10%	38	52	2.11	52	405.8
w/(c+sf) = 0.70						
3.0	0%	28	68	4.08	202	202.0
3.0	10%	96	Failed	1.20	148	81.1

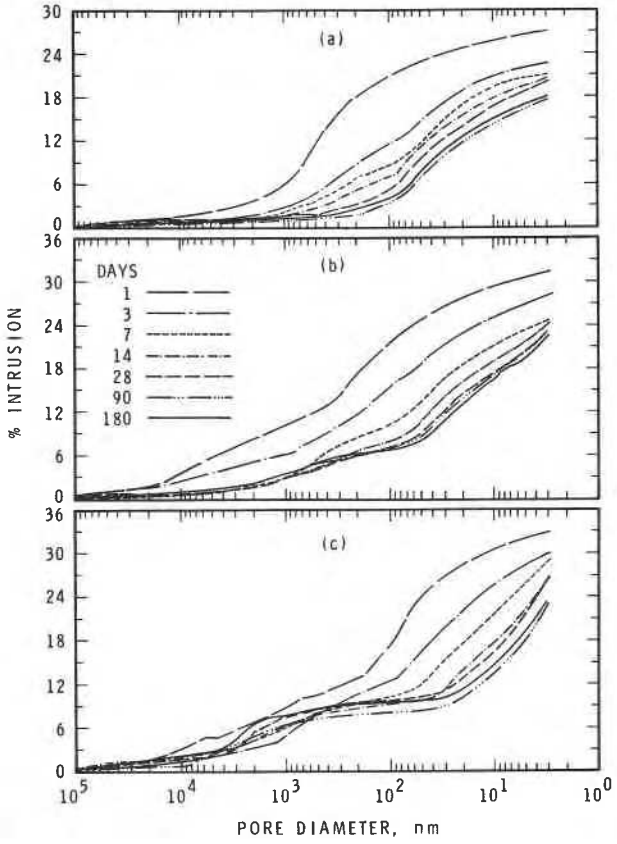

Fig. 1-- Pore-size distribution curves for cement mortar with different silica fume contents at different times (w/(c+sf) = 0.60). (a) 0 percent silica fume, (b) 10 percent silica fume, (c) 30 percent silica fume

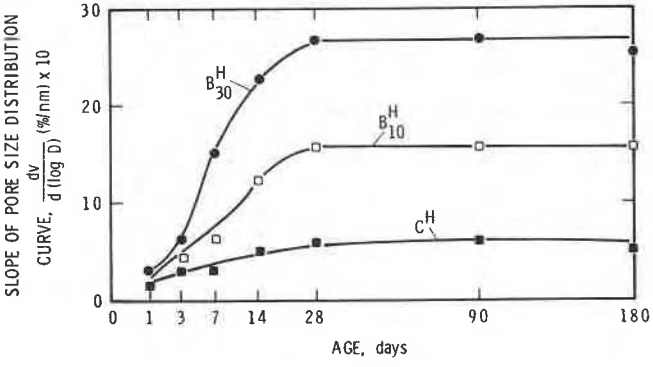

Fig. 2--Dependence of slope of pore-size distribution curve (at maximum intrusion pressure) on age and silica fume content

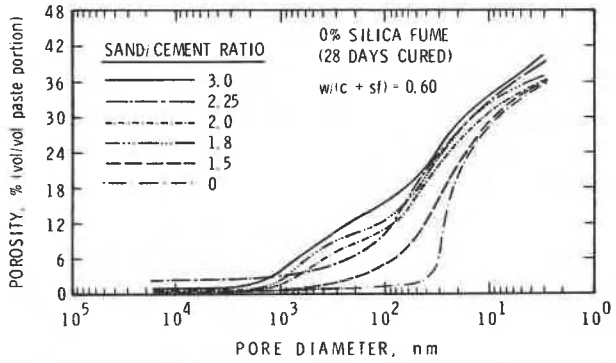

Fig. 3--Pore-size distribution of mortars as volume percent of volume of paste portion. Cured 28 days at w/c of 0.60. Silica fume = 0 percent. Sand/cement ratios 0.0→3.0

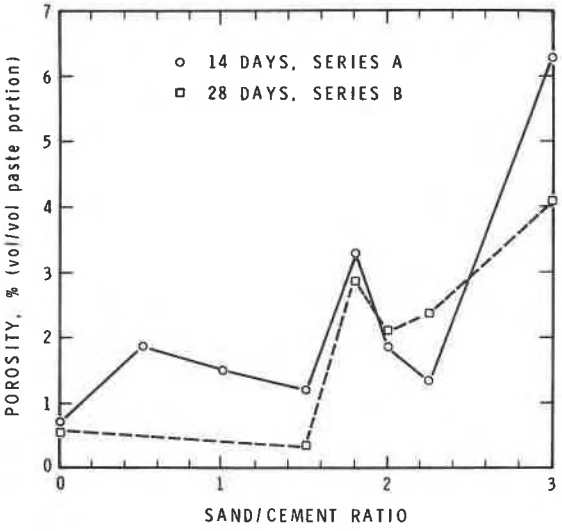

Fig. 4--Volume of pores of diameter 97→0.875 x 10^3 nm for mortars, sand/cement ratios 0.0→3.0, w/(c+sf) = 0.60, 0 percent silica fume

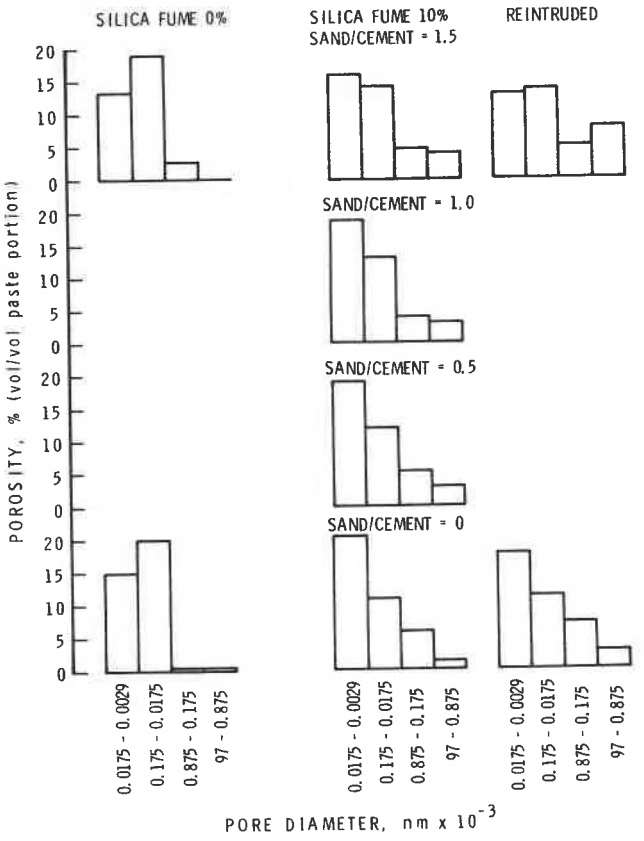

Fig. 5--Histograms of pore-size distribution of mortars, sand/cement ratio 0→1.5, w/(c+sf) = 0.60

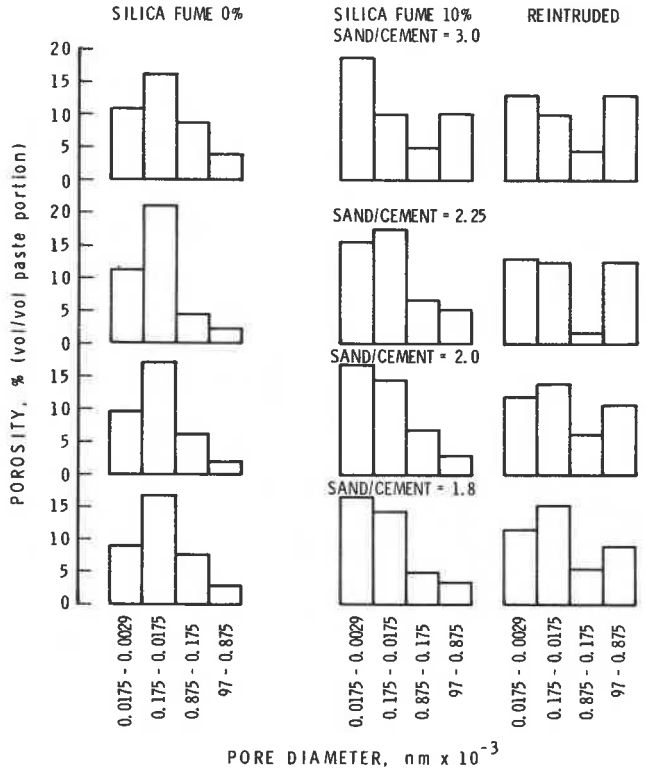

Fig. 6--Histograms of pore-size distribution of mortars, sand/cement ratio 1.8→3.0, w/(c+sf) = 0.60

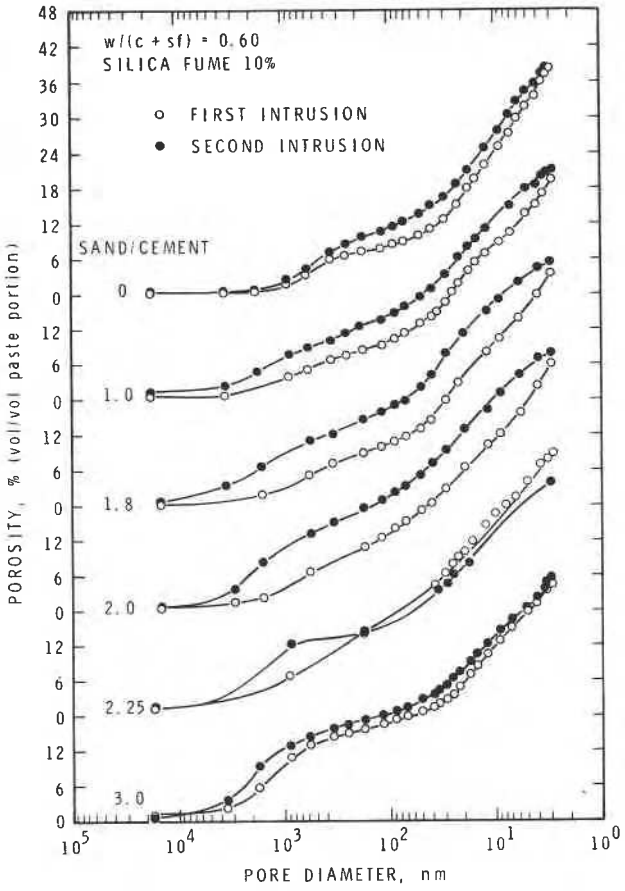

Fig 7--Pore-size distribution of mortars, first and second intrusions, containing 10 percent silica fume, sand/cement ratios 0→3.0, w/(c+sf) = 0.60